introduction to photoemission and application to layered oxides

Amal al-Wahish

Advance Solid state 672

Instructor: Elbio Dagotto

Spring 2009

Department of Physics and Astronomy,

University of Tennessee

wahish@utk.edu

(Dated: March 21, 2009)

Abstract

In this work we look at the introduction to photoemission and application to layered oxides and it's importance in the fields of surface science and condensed-matter. We present a historical introduction about photoemission , then review the general application of ARPES on layered oxides, and finally, we quote some modern applications.

I. INTRODUCTION

Modern photoelectron spectroscopy (PS), which often called "photoemission", offer a powerful widely-used way to study the properties of atoms, molecules, solids and surfaces[1, 2]. It is interesting to take a quick look at the history and demonstrate of the various stages of photoemission development.

A. Historical Introduction

Historically, the inspiration for Photoemission original essay came from Hertz works. In 1887 Hertz observed that a spark between two electrodes occurs more easily if the negative electrode is illuminated by UV radiation[3]. A few years later J.J. Thompson demonstrated that the effect was due to emission of electrons by the electrode while under illumination. The correct interpretation of this effect was given by Einstein (who was awarded the Nobel Prize in 1921 especially for his photoemission work). He postulated that light was composed of discrete quanta of energy E, this energy being proportional to ν, the frequency of the light. This energy, minus (ϕ+E_B) (where ϕ, the material work function, is measure of the potential barrier at the surface that prevents the valance electrons from escaping and the Binding energy)required to escape the solid, is taken up by the photoemitted electron, which thus escapes with a maximum kinetic energy $h\nu - \phi$,(ϕ for metals is typically around 4-5 eV for metals) [3, 4]. In recent years the energy resolution of this method has been improved considerably, namely for experiments using UV radiation to about 1meV, and in addition the energy resolution for experiments employing soft x-rays (15 keV) has reached values of about 50 meV. Where the X-ray Photoelectron spectroscopy(XPS) can be described with the three-step model:

1. Absorption of the x-ray inside the solid.

2.Transport of the excited photoelectron to the surface.

3. Escape of the photoelectron from the surface[5]. These Models will be explain briefly later.

This powerful method is relatively straight forward and allows to determine the energy and the momentum of electrons. The fundamental experiment in the photoelectron spectroscopy involves exposing the specimen to be studied to a flux of nearly monoenergetic

radiation with mean energy $E = h\nu$, and then observing the resultant emission of photoelectrons, and determine the kinetic energies of the electrons[1]. These steps can be done by using the Angular Resolved Photoemission Spectroscopy which provides rich information about the electron structure of crystals and of their surfaces[6].The following section demonstrated the ARPES.

B. Angle resolved Photoemission Spectroscopy

In the last two decades, angle-resolved photoemission spectroscopy (ARPES) has emerged as the most powerful probe of the momentum-resolved electronic structure of materials. This achievement has largely been due to the construction of new sources for synchrotron radiation and due to the extreme progress in the field of spectrometer design. The photoelectron spectrometers provide very high energy, momentum resolution at a single electron emission angle, and automated angle scanning techniques also facilitate a full hemisphere mapping of the electron distribution in momentum space. As a consequence, ARPES has now become a powerful imaging technique providing very direct k-space images of band dispersions as well as of constant energy surfaces. Moreover, in combination with synchrotron radiation as a tuneable photon source the experimental restrictions of ARPES regarding full k-space accessibility are strongly relaxed and it is possible to study three-dimensional electronic structures in great detail. In spite of the enormous potential of ARPES, however, there remains one disadvantage: the spatial resolution of the technique is generally limited to the spot size of modern light sources, i.e., generally to a few $100\mu m$. As one of the most important trends of photoemission spectroscopy, future efforts will tend to push down this limit by some orders of magnitude in order to be able to study the electronic properties of materials in the nanometer regime[4, 6].

In this work the experimental technique of photoemission imaging will be introduced and its accuracy will be discussed.

The general idea of an ARPES experiment is illustrated in Fig.1 Monochromatic light of a given energy $h\nu$ is absorbed by a crystalline material kept in ultra-high vacuum ($pressure < 5 * 10^{-11}$) and the intensity of the outgoing photoelectrons is measured as a function of their kinetic energy E_{kin} and emission angles . Via both energy and momentum conservation the measured quantities are directly related to the energy and momentum of the electrons inside

the crystal.

An ARPES sensor collects the photoelectrons Fig.2, provide information about the photoelectron energy, applying conservation laws of energy and momentum, where the energy and the momentum is conserved before and after the photoelectric effect.

$$E_{Kin} = h\nu - \phi - |E_B| \tag{1}$$

The crystal- momentum $\hbar k_{||}$ inside the solid

$$P_{\|} = \hbar k_{||} = \sqrt{(}2mE_{Kin}).\sin\theta \tag{2}$$

Where $P_{\|}$ is the parallel" the direction due to the surface of the crystal sample" components of the momentum of the ejected electrons which approximately equals the momentum of the electrons in the solid. This is the reason why the sensor only measure the parallel momentum, where the perpendicular components break the conservation of the momentum due to lack of translational symmetry along the surface. In addition the momentum of the incoming photons is negligible compared to the momentum of the electrons. In the low-dimensional systems characterized by anisotropic electronic structure and a negligible dispersion along the z-axis, the parallel component of the wave vector $\mathbf{k}$ is enough to determined the electronic dispersion in this particular case [2, 4]

Hüfner sketch fig.3 the energetic of the photoemission process in 1995, where the electron energy distribution produced by incoming photons and measured as a function of the kinetic energy E_{kin} of the photoelectrons (right) is more conveniently expressed in terms of the binding energy E_B when one refers to the density of states inside the solid (left), where N(E) is the electronic density state inside the solid.[2, 4]

In this work ARPES can be demonstrated by taking two cases. First a layered compounds of copper Oxide superconductor, second Ion-based superconductor.

Mapping out the electronics dispersion relations $E(\mathbf{k}_{\|})$ by tracking the energy position of the peaks of ARPES spectral at various angles to achieve higher energy and momentum resolution .

$$\Delta\mathbf{k} \simeq \sqrt{(}2mE_{Kin}/\hbar^2).cos\theta\Delta\theta \tag{3}$$

Where $\Delta\theta$ correspond to finite acceptance angle of the electron analyzer.

II. A SUMMARY OF THREE STEP MODEL

The three step model developed on ARPES from solid by Berglund and Spicer. This model breaks up the EP process into three steps, the three step model is sketched by Hüfner fig.4. The photocurrent is decomposed into three separate factors: the probability of excitation in the bulk solid, the probability of scattering of the excited electron on its path to the surface by the atoms constituting the solid, and the probability of transmission through the surface potential barrier for its final acceptance in the detector[6]. The optical excitation of the electron in the bulk contains the all information about the intrinsic electronic structure of the material.Travel of the excited electron to the surface can be described in terms of an effective mean free path, proportional to the probability that the excited electron will reach the surface without inelastic scattering processes, this processes determine the surface sensitivity of the photoemission, where The suitability of PS to surface studies of materials is essentially due to the short inelastic attenuation length of the photoelectrons in the sample, as shown in Fig.5, where the so called universal curve for electron attenuation lengths in a large number of elemental samples as a function of electron kinetic energy is shown[**?**]. Also the scattering process give rise to a continuous background in the spectra which is usually ignored or subtracted. The Escape of the photoelectron into vacuum, is described by a transmission probability through the surface, which depends on the energy of the excited electron as well as the material work function ϕ. the photoelectron wave function can be expressed as

$$\psi(r) = \int \mathrm{d}r' G^r(r, r') V_I(r') \;\; \psi_i(r') \tag{4}$$

where V_i describes the perturbation of the external light, ψ_i is the initial state one-electron wave function of energy E_i, and is the Green function of the solid at the photoelectron energy $E_i + \hbar\omega$,

$$G^r(r, r') = \sum_f \frac{{\psi_f}^*(r')\,\psi_f(r)}{E_i + \hbar\omega - E_f + \mathrm{i}\delta} \tag{5}$$

III. GOLDEN RULE

A. Linear response in the external field

The Hamiltonian of one electron in a system described by a potential $V(r)$, to which an external electromagnetic field is applied

$$H = \frac{p^2}{2m} + V(r) - \frac{e}{2m}[A(r).p + p.A(r)] + \frac{e^2}{2m}|A(r)|^2 \tag{6}$$

where p is the electronic momentum operator.$A(r)$ is the vector potential associated with the field. A common choice is to work in the Coulomb gauge, in which

$$\nabla.A(r) = 0 \tag{7}$$

Actually when the ultraviolet being used the momentum and the electromagnetic vector potential are commute

$$(A(r).p + p.A(r)) = \mathrm{i}\hbar\nabla.A(r) = 0 \tag{8}$$

The interaction potential V_I can thus be expressed as

$$V_I(r) = -\frac{e}{m}[A(r).p] + \frac{e^2}{2m}|A(r)|^2 \tag{9}$$

The interaction with the photon is treated as a perturbation given by

$$H_{\text{int}} = -\frac{e}{m}[A(r).p] \tag{10}$$

For low intensities of the external field, first order perturbation theory can be used to study the interaction between the electromagnetic radiation and the system. Thus, applying the Golden Rule to calculate the photocurrent, we obtain:

$$I(f) = |M_{\text{if}}|^2 = |\langle\psi_f|V_I|\psi_i\rangle|^2 \tag{11}$$

The most important approximations introduced in the theoretical formalism are the restriction to a one-electron picture, and the use of only first-order perturbation theory to calculate the interaction between the incident radiation and the system. The latter approximation is equivalent to neglecting terms of order $\approx |A|^2$ in the calculation of the photocurrent, so the term of order $\approx |A|^2$ in the interaction potential V_I is omitted. This approximation remains

valid provided that the flux of incident photons is relatively low. The matrix element M_{if} after keeping only the lowest-order terms can be written as:

$$M_{\text{if}} = \langle \psi_f | H_{\text{int}} | \psi_i \rangle = \frac{ie\hbar}{\text{mc}} \langle \psi_f | A(r).\nabla | \psi_i \rangle \tag{12}$$

B. Dipole approximation

Dipole approximation is theoretical description of the interaction between the electromagnetic field and the system. The dipole approximation assumes that the variation of the external field $A(r)$ is small in the spatial region in which the matrix element M_{if} is not negligible. the external electromagnetic field is periodic in space, it can be expressed as:

$$\mathbf{A}(r) = A_0 \mathbf{e}\ e^{i\mathbf{k}\cdot\mathbf{r}} = A_0 \mathbf{e}(1 + i\mathbf{k}\cdot\mathbf{r} + \ldots) \tag{13}$$

where A_0 is the complex amplitude of the field (a scalar number), e is a unitary vector in the direction of the light polarization, and k is a vector pointing in the propagation direction of the field. The dipole approximation consists in keeping only the first term of this expansion in the calculation of the photocurrent via Eq. (11) (it is assumed that $|kr| \ll 1$)[6].

The matrix element in the dipole approximation can be written as

$$M_{\text{if}} = \frac{ie\hbar}{mc} \mathbf{A}_0 \langle \psi_f | \mathbf{e}.\nabla | \psi_i \rangle \tag{14}$$

the momentum operator $\hat{\mathbf{p}}$ can be written as the commutator of two other operators

$$\hat{\mathbf{p}} = -i\hbar\hat{\nabla} = \frac{-im}{\hbar}[\hat{r}, \hat{H}_0] \tag{15}$$

Hence, if ψ_i and ψ_f are eigenstates of the Hamiltonian H_0, the length form of the matrix element M_{if} can be calculated

$$M_{\text{if}} = \frac{-ie}{\text{c}\hbar} \mathbf{A}_0 \, (E_f - E_i) \langle \psi_f | \mathbf{e}.r | \psi_i \rangle \tag{16}$$

A third form, known as the acceleration form of the matrix element:

$$M_{\text{if}} = \frac{-ie\hbar}{mc} \frac{A_0}{(E_f - E_i)} \langle \psi_f | \mathbf{e}.(\nabla.V) | \psi_i \rangle \tag{17}$$

To find these matrices, the following identity has been used

$$\langle \psi_f | \nabla | \psi_i \rangle = \frac{1}{(E_f - E_i)} \langle \psi_f | [H, \nabla] | \psi_i \rangle = \frac{-1}{(E_f - E_i)} \langle \psi_f | \nabla V | \psi_i \rangle \tag{18}$$

For a single atom, the dipole approximation leads to certain selection rules in the symmetry of the photoemitted electron wavefunction. These selection rules derived by expanding the wavefunctions in the basis set of spherical harmonics. The expansions of the wavefunctions and the dipole operator can be introduced into Eq. (16) to obtain the matrix element as[6]:

$$M_{\mathrm{if}} = \frac{-ie}{\mathrm{c}\hbar}\mathbf{A}_0\left(E_f - E_i\right)\left(\frac{4\pi}{3}\right)^{\frac{1}{2}}\sum_{l_f,m_f}\left\{\int drr^3\left[R^f_{l_f m_f}(r)\right]^* R^i_{l_i m_i}(r)\right\}\times\int d\Omega_r Y^*_{l_f m_f}\left(\Omega_r\right)Y_{10}\left(\Omega_r\right)Y_{l_i m_i}\left(\Omega_r\right) \tag{19}$$

The integral over angles Ω_r determines the allowed symmetries for the final states. According to general properties of the spherical harmonics, this integral is different from zero only if $l_f = l_i 1$and $m_f = m_i$.

The total photoemission intensity measured as a function of E_{kin} at a momentum k, $I(k, E_{kin})$is proportional to

$$\sum_{f,i}|M^k_{\mathrm{f,i}}|^2\sum_m|\langle\psi^{N-1}_m|\psi^{N-1}_i\rangle|^2\,\delta\left(E_{\mathrm{Kin}} + E^{N-1}_m - E^N_i - \mathrm{h}\nu\right) \tag{20}$$

$$|C_{m,i}|^2 = |\langle\psi^{N-1}_m|\psi^{N-1}_i\rangle|^2 \tag{21}$$

$|C_{m,i}|^2$ is the probability that the removal of an electron from state i

From this we can see that, if $\psi^{N-1}_i = \psi^{N-1}_{m_0}$ for one particular state$m = m_0$, then the corresponding $|C_{m_0,i}|^2$ will be unity and all the other $C_{m,i}$ zero; in this case, if $M^k_{\mathrm{f,i}} \neq 0$, the ARPES spectra will be given by a delta function at the Hartree-Fock orbital energy $E^k_B = -\epsilon_k$, as shown in Fig. 6(b) (i.e., the noninteracting particle picture). In strongly correlated systems, however, many of the $|C_{m,i}|^2$ will be different from zero because the removal of the photoelectron results in a strong change of the systems effective potential and, in turn, ψ^{N-1}_i will overlap with many of the eigenstates $\psi^{N-1}_{m_0}$. Thus the ARPES spectra will not consist of single delta functions but will show a main line and several satellites according to the number of excited states m created in the process Fig.6(c)[4].

IV. APPLICATION

The investigation of the hightemperature superconductors such as copper oxide and Ione based superconductor, ARPES proved to be very successful in detecting dispersive electronic features. The configuration of a generic angle-resolved photoemission beamline is shown in

Fig. 7. A beam of white radiation is produced in a wiggler or an undulator (these so-called insertion devices are the straight sections of the electron storage ring where radiation is produced), is monochromatized at the desired photon energy by a grating monochromator, and is focused on the sample. Alternatively, a gas-discharge lamp can be used as a radiation source (once properly monochromatized, to avoid complications due to the presence of different satellites and refocused to a small spot size, essential for high angular resolution). Photoemitted electrons are then collected by the analyzer, where kinetic energy and emission angle are determined, see the System for ARPES fig 8. A conventional hemispherical analyzer consists of a multielement electrostatic input lens, a hemispherical deflector with entrance and exit slits, and an electron detector (i.e., a channeltron or a multichannel detector). The heart of the analyzer is the deflector, which consists of two concentric hemispheres of radius R_1 and R_2 . These are kept at a potential difference ΔV, so that only those electrons reaching the entrance slit with kinetic energy within a narrow range centered at the value $E_{pass} = e\Delta \mathrm{V}/\left(\frac{R_1}{R_2} - \frac{R_1}{R_2}\right)$ will pass through this hemispherical capacitor, thus reaching the exit slit and then the detector. In this way it is possible to measure the kinetic energy of the photoelectrons with an energy resolution given by $\Delta E_a = E_{pass}\left(\frac{w}{R_0} + \frac{\alpha^2}{4}\right)$,where$R_0 = (R_1 + R_2)/2$,w is the width of the entrance slit, and α is the acceptance angle. The role of the electrostatic lens is to decelerate and focus the photoelectrons onto the entrance slit. By scanning the lens retarding potential one can effectively record the photoemission intensity versus the photoelectron kinetic energy. It is thus possible to measure multiple energy distribution curves simultaneously for different photoelectron angles, obtaining a 2D snapshot of energy versus momentum Fig.9[4].From figure9, it very clear that energy (ω) vs momentum ($k_{\|}$) image plot of the photoemission intensity from $Bi_2Sr_2CaCu_2O_{8+\delta}$ along $(0,0) - (\pi,\pi)$. This k-space cut was taken across the Fermi surface (see sketch of the 2D Brillouin zone upper left) and allows a direct visualization of the photohole spectral function $A(k,w)$ (although weighted by Fermi distribution and matrix elements). The quasiparticle dispersion can be clearly followed up to E_F , as emphasized by the white circles. Energy scans at constant momentum (right) and momentum scans at constant energy (upper right) define energy distribution curves (EDCs) and momentum distribution curves (MDCs), respectively. Ione based superconductor is another application to ARPES, where in 2006 a Japanese group discovered Iron-based superconductors Such as: LaOFeP ($Tc = 5.9K$) and LaOFeAs (Tc = 26 K , fluoride-doped), the Japanese researchers

discovered earlier (August 2008), that a new class of iron-based superconducting materials also had much higher transition temperatures than the conventional low-temperature superconductors. $SmO_{0.9}F_{0.1}FeAs$, being 55 K. In September 2008, Shens group studied the electronic structure of LaOFeP. The purpose of this study was to understand the nature of the ground state of the parent compounds LaOFeP, and to reveal the important differences between Iron Oxypnictide and Copper based superconductors, all these study was depend on ARPES technique, graph 10 show the powerful of this technique compar to theoretical approach, Local-density approximations (LDA).

V. CONCLUSION AND SUMMARY

1-The photoemission process from a core level can be described as the photoexcitation from a single atom, followed by the transport of the photoelectron on its way to the detector.2- Angle resolve photoemission spectroscopy (ARPES) aka. k-space microscopy is a direct measurement of the quasiparticle band dispersion , i.e. energy versus momentum.3- The ARPES technique: a-By measuring the K.E and angular distribution of the electrons photoemitted from a sample illuminated, one can gain information on both, the energy and momentum.b-Very useful for detecting bands and Fermi Surface c-Gives us information about the bulk and surface electronic structure and superconductor gap of materials. d-Provides us direct and valuable information about the electronic states of a solid. e-Allows us to compare directly with the theory. f-One can have high resolution information on both energy and momentum.

[1] C. Fadley, *Basic Cncept of X-ray Photoelectron Spectroscopy* (Dapartment of Chemistry, University of Hawaii, Honolulu, Hawaii, 1978).

[2] S. Hufner, *Very High Resolution Photoelectron Spectroscopy,Lecture Notes in Physics 715* (Springer, Berlin, Heidelberg, 2007), 1st ed.

[3] P. Y. Y. M. Cardona, *Fundementals of Semiconductors physics and Materials properties* (Springer, Berline, Germany, 2005), 3rd ed.

[4] Z.-X. S. Andrea Damascelli, Zahid Hussain, Reviews of Modern Physics **75**, 473 (2003).

[5] A. K. Frank de Groot, *Core level Spectroscopy of Solids* (CRC Press, Taylor and Francies Group, USA, 1964), 1st ed.

[6] M. A. H. Wolfgang Schattke, *Solid-State Photoemission and related Methods, theory and experiment* (WiLey-Vch GmbH and Co.KGaA, Weinheim, Germany, 2003), 1st ed.

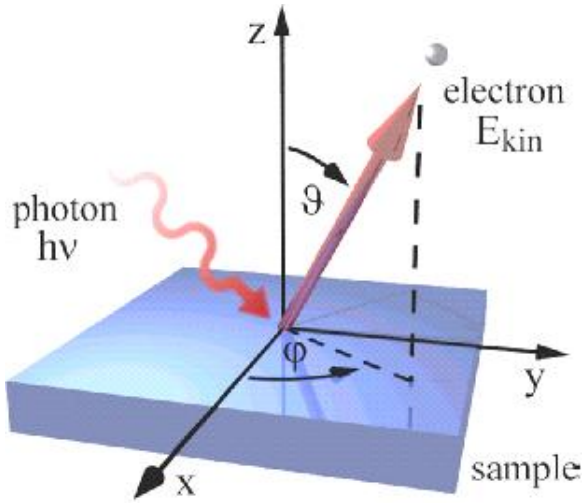

FIG. 1: In ARPES, measuring the energy and momenta (mass times velocity) of electrons ejected from a sample struck by energetic photons makes it possible to calculate the electrons' initial energy and momenta, and from this determine the sample's electronic structure.

FIG. 2: The ARPES sensor now sits inside the vacuum chamber. This picture was taken before it was completely built.

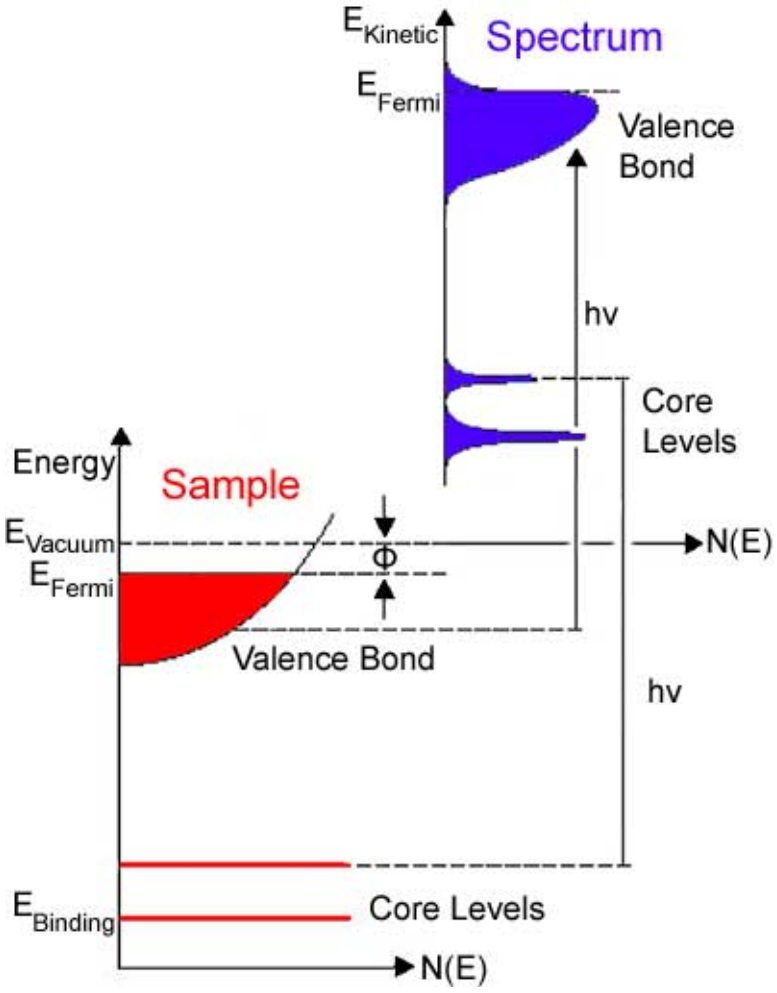

FIG. 3: The ARPES sensor, displayed as "Spectrum" in blue, displays the intensity of detected electrons, N(E), that have various kinetic energies, E. These values obtained by the ARPES sensor correspond to the actual values of the "Sample", displayed red. In a solid material, the electrons are distributed to an energy level below EFermi, the Fermi Level. The ARPES spectrum reveals peaks with an identical energy distribution as the one in the solid. However, the peaks are slightly wider, due to electron scattering during the process.

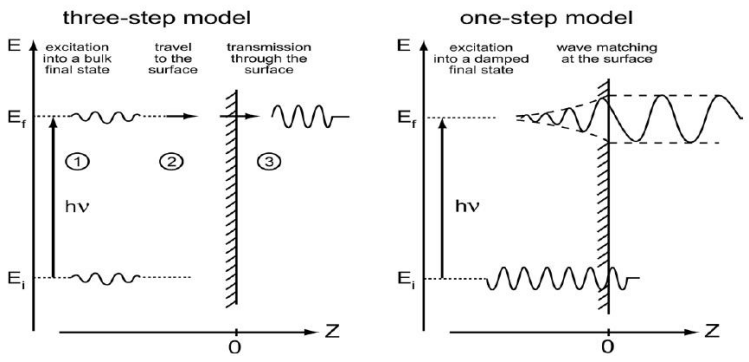

FIG. 4: Pictorial representation of three-step and one-step model descriptions of the photoemission process.

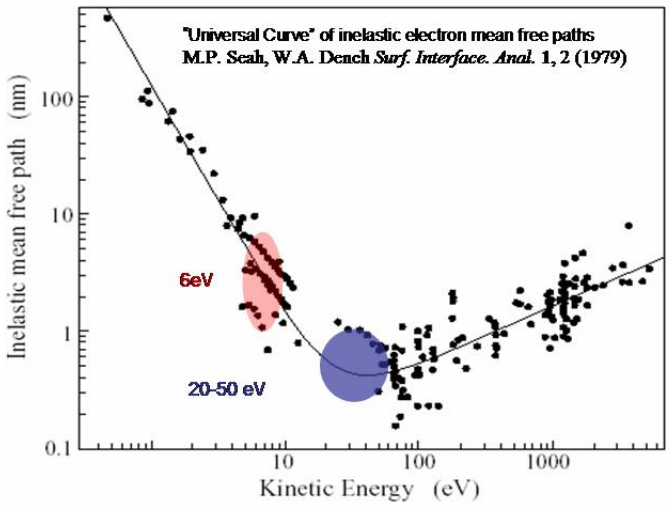

FIG. 5: Illustration of the universal curve for electron attenuation in solids as a function of electron kinetic energy

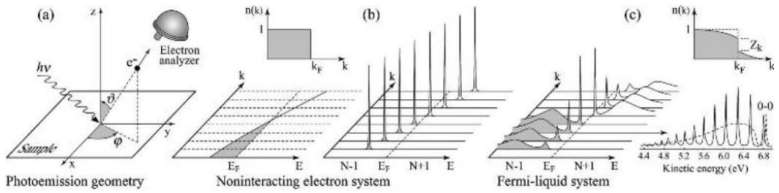

FIG. 6: Angle-resolved photoemission spetroscopy: (a) geometry of an ARPES experiment in which the emission direction of the photoelectron is specified by the polar (q) and azimuthal (w) angles; (b) momentum-resolved one-electron removal and addition spectra for a noninteracting electron system with a single energy band dispersing across EF ; (c) the same spectra for an interacting Fermi-liquid system (Sawatzky, 1989; Meinders, 1994). For both noninteracting and interacting systems the corresponding groundstate (T50 K) momentum distribution function n(k) is also shown. (c) Lower right, photoelectron spectrum of gaseous hydrogen and the ARPES spectrum of solid hydrogen developed from the gaseous one (Sawatzky, 1989).

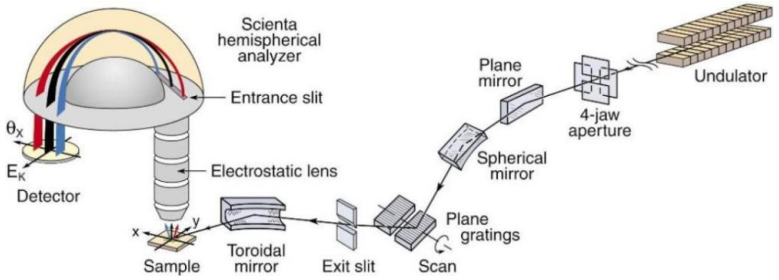

FIG. 7: Generic beamline equipped with a plane grating monochromator and a Scienta electron spectrometer (Color).

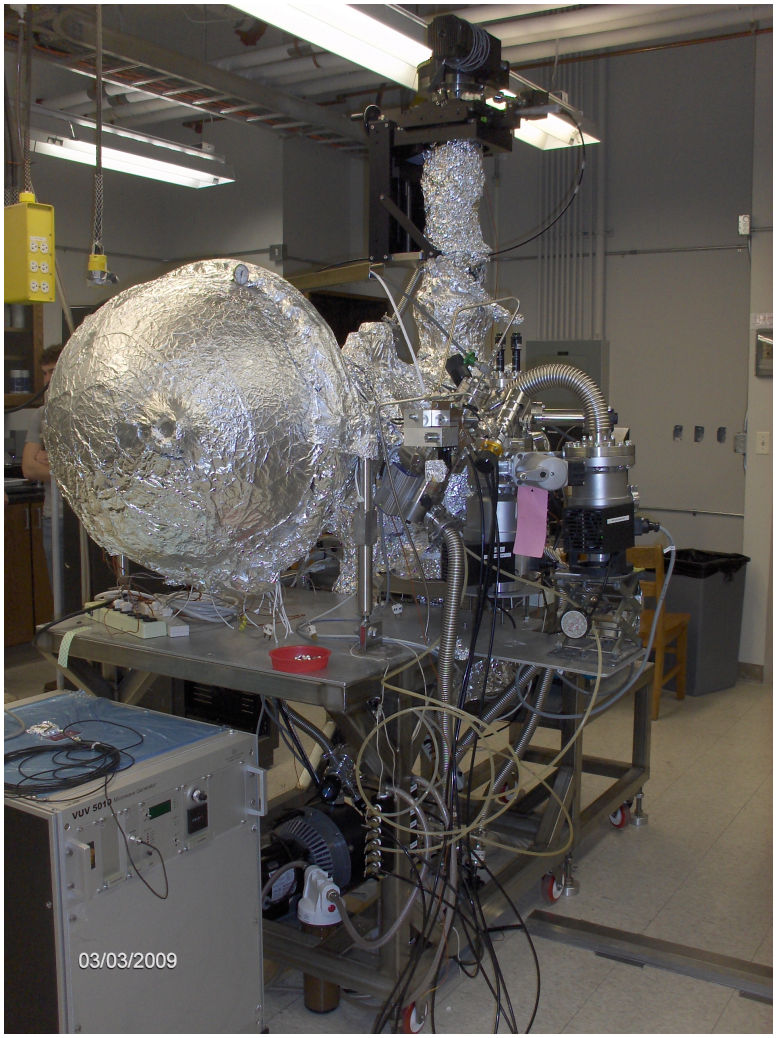

FIG. 8: Photoemission Spectroscopy's system, Mannella's lab,UTK.

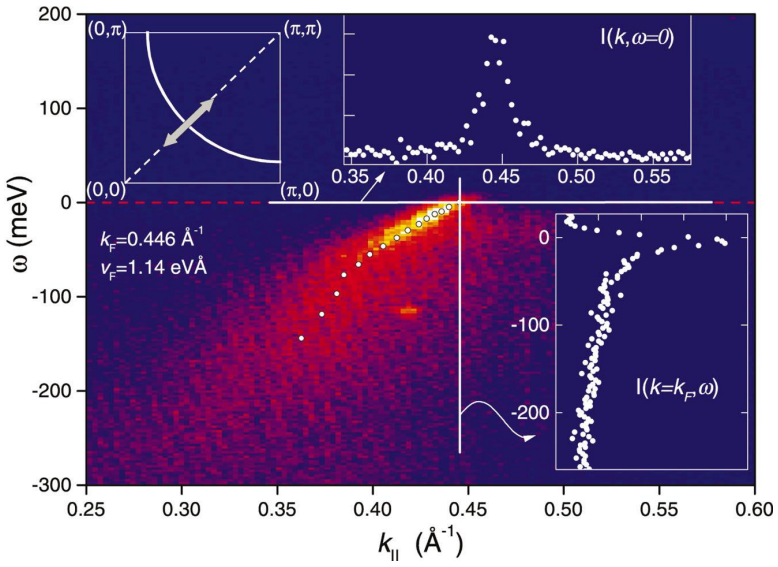

FIG. 9: Energy (ω) vs momentum $k_{||}$ image plot of the photoemission intensity from $Bi_2Sr_2CaCu_2O_{8+\delta}$ along $(0,0)$-(π,π). This k-space cut was taken across the Fermi surface (see sketch of the 2D Brillouin zone upper left) and allows a direct visualization of the photohole spectral function $A(k,v)$ (although weighted by Fermi distribution and matrix elements). The quasiparticle dispersion can be clearly followed up to E_F , as emphasized by the white circles. Energy scans at constant momentum (right) and momentum scans at constant energy (upper right) define energy distribution curves (EDCs) and momentum distribution curves (MDCs), respectively.

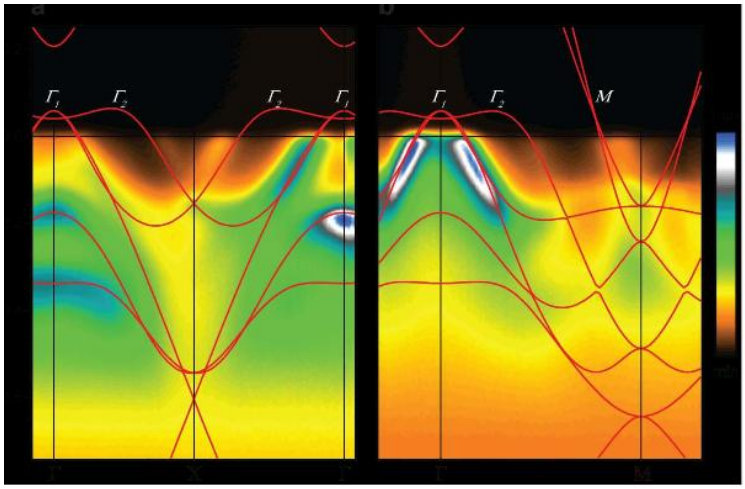

FIG. 10: Comparison between angle-resolved photoemission spectra and LDA band structures along two high-symmetry lines. ARPES data from LaOFeP (image plots) were recorded using 42.5-eV photons with an energy resolution of 16 meV and an angular resolution of 0.3u